

ORIGINAL ARTICLE

Prenatal and postnatal presentation of *PRMT7* related syndrome: Expanding the phenotypic manifestations

Roe Birnbaum^{1,2†} | Naama Yosha-Orpaz^{3,4†} | Miri Yanoov-Sharav^{3,5} | Dvora Kidron^{6,2} | Hila Gur⁷ | Keren Yosovich^{3,7} | Tally Lerman-Sagie^{2,3,4} | Gustavo Malinger^{1,2} | Dorit Lev^{2,3,5} 

¹OB-GYN Ultrasound Unit, Lis Maternity Hospital, Tel Aviv Medical Center, Tel Aviv, Israel

²Sackler School of Medicine, Tel Aviv University, Tel-Aviv, Israel

³Metabolic Neurogenetic Service, Holon, Israel

⁴Pediatric Neurology Unit, Holon, Israel

⁵The Rina Mor Institute of Medical Genetics, Wolfson Medical Center, Holon, Israel

⁶Pathology Department, Sapir Medical Center, Kfar Saba, Israel

⁷Molecular Genetics Laboratory, Wolfson Medical Center, Holon, Israel

Correspondence

Dorit Lev, The Rina Mor Institute of Medical Genetics, Wolfson Medical Center, POB 5, Holon 58100, Israel.

Email: dorlev@post.tau.ac.il

Protein arginine methyltransferase 7 (*PRMT7*) is a member of a family of enzymes that catalyze the transfer of methyl groups from S-adenosyl-L-methionine to nitrogen atoms on arginine residues. Arginine methylation is involved in multiple biological processes, such as signal transduction, mRNA splicing, transcriptional control, DNA repair, and protein translocation. Currently, 10 patients have been described with mutations in *PRMT7*. The shared findings include: hypotonia, intellectual disability, short stature, brachydactyly, and mild dysmorphic features. We describe the prenatal, postnatal, and pathological findings in two male sibs homozygote for a mutation in *PRMT7*. Both had intrauterine growth restriction involving mainly the long bones. In addition, eye tumor was found in the first patient, and nonspecific brain calcifications and a systemic venous anomaly in the second. The pregnancy of the first child was terminated and we describe the autopsy findings. The second child had postnatal growth restriction of prenatal onset, hypotonia, strabismus, sensorineural hearing loss, genitourinary and skeletal involvement, and global developmental delay. He had dysmorphic features that included frontal bossing, upslanting palpebral fissures, small nose with depressed nasal bridge, and pectus excavatum. Our patients provide additional clinical and pathological data and expand the phenotypic manifestations associated with *PRMT7* homozygote/compound heterozygote mutations to include brain calcifications and delayed myelination, and congenital orbital tumor.

KEYWORDS

developmental delay, pilocytic astrocytoma, prenatal ultrasound, *PRMT7*, systemic venous anomaly

1 | INTRODUCTION

In 2015, Akawi et al. (2015) described six affected individuals from three families with variants in the protein arginine methyltransferase 7 (*PRMT7*) gene. The patients were part of a cohort of 4,125 families analyzed according to probabilistic genotype and phenotype matching, which gave rise to new genes. The associated clinical phenotype seen in these patients was considered a phenocopy of pseudohypoparathyroidism (PHP; MIM 103580; also known as Albright hereditary osteodystrophy). In 2017, Kernohan et al. (2017) reported a 6-year-old male with severe intellectual disability, facial dysmorphism, microcephaly, short stature, brachydactyly, cryptorchidism, and seizures

who was diagnosed with a homozygous 15,309 bp deletion encompassing the transcription start site of the *PRMT7* gene. Agolini et al. (2018) described three additional patients with severe/moderate intellectual disability, short stature, brachydactyly, and mild dysmorphic features. Recently, Valenzuela et al. (2018) described a 2-year-old girl with intellectual disability, facial dysmorphism, short stature, brachydactyly, and hearing loss with two mutations in *PRMT7*. In this report, we describe the prenatal, postnatal, and pathological findings of two male sibs found to harbor a homozygous *PRMT7* mutation.

2 | PATIENTS AND METHODS

This is a retrospective analysis of data from two consecutive pregnancies. The study was approved by the institutional review board. The

[†]These authors contributed equally to this work.

first pregnancy include the prenatal ultrasound (US) findings (Voluson E8, 5–9 MHz and 6–12 MHz vaginal transducers, 4–8 MHz abdominal transducer, GE, Austria) and the pathologic post mortem exam results. The second includes the prenatal US findings and data from the post-natal clinical follow-up of the live born child. In addition, we describe the genetic analysis performed in both patients according to the following protocol; we obtained genomic DNA from the patients' peripheral blood by the QIAamp DNA Mini kit (QIAGEN), according to the manufacturers' instructions. We performed whole exome sequencing (WES) analysis on the patients' DNA; the sample was enriched with Sureselect Human All Exome v.5 kit 50 Mb (Agilent, Santa Clara, CA). Sequencing was carried out on HiSeq4000 (Illumina, San Diego, CA) as 100-bp paired-end runs. Reads were aligned with the human reference genome (assembly GRCh37/hg19). Pipeline was performed using the Genoox platform based on BWA (version 0.7.16) for read alignment and GATK HaplotypeCaller (version 3.7) and FreeBayes (version 1.1.0) for variant calling. Dataset files including the annotated information were analyzed according to the following filtering steps: variants which were called less than 9 times and synonymous variants were removed. Variants were filtered based on allele frequency less than 0.01 according to online databases; dbSNP, 1000G, ExAC, and gnomAD. Likely pathogenicity was assessed if the variant was truncating (splicing or nonsense), missense or an in-frame indel. Missense and in-frame indels were considered if they were predicted to be pathogenic by online prediction tools, PolyPhen-2, SIFT, and Mutation Taster. Conformation and family segregation were performed using direct Sanger sequencing (3500 Genetic Analyzer Applied Biosystems). A written informed consent was obtained from the patients parents, in accordance with the hospitals ethics committee standards.

2.1 | Patient I-2

A 31-year-old patient, G2P1, with no prior medical history. The patient and her husband, both of Jewish Bucharian origin, were referred to our prenatal US unit at 34 weeks of gestation, because of fetal growth restriction (FGR). Obstetric history included one vaginal delivery of a healthy child at term who is 6 years old and healthy. Follow-up during the current pregnancy included low risk first trimester screen test ($NT = 1.1$ mm) and low risk second trimester integrated screen test, and a normal anatomic US scan at 15 weeks. The second trimester morphologic US examination performed at 23 weeks was considered normal but the estimated fetal weight (EFW) was 508 g. which corresponds to the 11th percentile according to Hadlock (Hadlock, 1990). Amniocentesis was not performed. At 31 weeks, the fetus appeared growth restricted, with EFW below the first percentile with normal Doppler indices. Fetal echocardiography performed at that time was considered normal. At 31 weeks, the EFW was 1,217 g. (below the first centile according to Hadlock) with normal Doppler indices. Fetal echocardiography was normal.

We examined the patient for the first time at 34^{5/7} weeks and found severe FGR, with an abdominal circumference below the first percentile, femur, and tibia length were 3.5 and 2.7 standard deviations (SD) below the mean for gestational age, respectively (Chitty & Altman, 2002). Head circumference was within the normal range, and all Doppler indices were normal. Inside the left orbit, we identified a retrobulbar

lesion, comprising of both solid and cystic components (Figure 1a). Color Doppler demonstrated vascularization within the mass. There was left microphthalmia with an anterior–posterior diameter of 11 mm, compared to 17 mm of the normal right eye. A lucent lens was imaged but the optic nerve sheath could not be clearly visualized. During periods of eye movements, the lesion was visualized moving in conjunction with the eye. Post mortem fetal karyotype and chromosomal micro array were normal. On pathological examination, the fetal weight was 1970 g. A solid tumor with cystic components was found occupying the posterior part of the left orbit, behind a distorted eye. Histologically, the tumor cells appeared elongated with a fibrillated background, these cells were positive for glial fibrillary acidic protein (GFAP) and Vimentin immunohistochemistry stains, and negative for s100, neurofilaments, EMA, and CD34; these findings were consistent with the diagnosis of juvenile pilocytic astrocytoma (PA). The brain macroscopic anatomy was normal; however microscopic examination revealed a few clusters of periventricular necrosis with calcified axons and a glial reaction. A retrospective analysis of the US images showed the presence of few periventricular echogenic foci (Figure 1b).

2.2 | Patient I-3

During her next pregnancy, the patient was referred at 23 weeks. Prior to referral she had a normal nuchal translucency test with an integrated screen test result of 1:40 risk for trisomy 21. The two morphologic scans showed normal fetal anatomy, but at the 21 week scan the fetal weight estimation was at the fifth percentile, with femur length measured 2.4 SD below the norm (Chitty & Altman, 2002). The 23 week scan we performed showed a fetal weight estimation at the 10th percentile with short long bones, between 2.5 and 3.5 SD below the norm for all bones. An interrupted inferior vena cava with azygos continuation was diagnosed, without additional cardiac malformations supporting a heterotaxy syndrome. Fetal karyotype and chromosomal microarray were normal; the common mutations in the FGFR3 gene associated with Achondroplasia were not detected. A growth follow-up US performed at 29 weeks, showed that fetal weight was below the first percentile, and the femur and humerus bones length were 3.3 and 3.2 SD below the mean, respectively. At 35 weeks, transvaginal targeted brain ultrasound demonstrated isolated periventricular echogenic foci at the level of the anterior horns (Figure 1c). During follow-up, we counseled the couple regarding the high probability for an unfavorable prognosis resulting from a syndromic etiology, although a definitive diagnosis could not be reached. The couple decided to continue the pregnancy. Delivery was at 37^{5/7} weeks, spontaneous, vaginal, and uncomplicated. Birth weight was 1,717 g.(–4 SD) and the head circumference was 30.5 cm (10th centile) with a normal Apgar score. Postnatally, a unilateral undescended testes and a penile chordee were observed. Brain US scans at the age of 1 and 6 days showed mild periventricular leukomalacia. Because of the US images, the low birth weight, and transient thrombocytopenia, a urine test for cytomegalovirus was performed and was negative. Maternal serology for other TORCH viruses was also negative. Brain MRI at the age of 7 months showed mild dysmorphic changes of the anterior horns and the lateral ventricles, subtle periventricular calcifications and delayed myelination (Figure 2a,b). The spinal cord ended at a low position (L3–L4) with no intervening lesion or fat

TABLE 1 Common clinical features and molecular data from previously published studies and our patients

	Akawi et al. (2015)	1	2	3	4	5	6	7	8	9	10	11	12	13
								Kernohan et al. (2017)	Agolini et al. (2018)			Valenzuela et al. (2018)		This report
Mutations	c.1276-1G>A			c.95G>C; p.Arg32Thr	c.95G>C; p.Arg32Thr			15,309bpdel 16:68345747- 68361056	c.322G>T p.Glu108Ter	c.1490G>A p.Arg497Gln		c.431_432 del 1246dupGCTCTCCG	c.1074_1075delAG p.Arg358Fs	
	c.1480T>C; p.Trp494Arg			c.1159A>G; p.Arg387Gly	c.1056-1G>T									
Zygosity	Compound heterozygous	Compound heterozygous	Compound heterozygous	Compound heterozygous	Compound heterozygous	Compound heterozygous	Compound heterozygous	Homozygous	Homozygous	Homozygous	Homozygous	Homozygous	Homozygous	Homozygous
IUGR								✓	✓			✓	✓	✓
SGA	✓	✓			NA	NA	NA	✓	✓			✓	✓	NA
Microcephaly			✓PN	✓PN	✓PN	✓PN	✓C	✓C	✓C					NA
Hypotonia	✓	✓	✓	✓	✓	✓	✓	✓	✓	✓	✓	✓	✓	NA
Feeding difficulties								✓	✓					NA
Dysmorphism	✓	✓	✓	✓	✓	✓	✓	✓	✓	✓	✓	✓	✓	✓
Brachydactyly	✓	✓	✓	✓	✓	✓	✓	✓	✓	✓	✓	✓	✓	NA
Sensorineural hearing loss	✓													NA
Strabismus														NA
Short stature	✓	✓	✓	✓	✓	✓	✓	✓	✓	✓	✓	✓	✓	NA
FTT/obesity	OB	OB	OB	OB	OB	OB	OB	FTT	FTT	OB		FTT	FTT	NA
GU abnormalities	✓							✓					✓	
ID	LD	LD	Mild	Mild	Mild	Mild	Mild	Sev.	Sev.	Mod.	Mod.	Mild	Mild	NA
Seizures	✓							✓	✓	✓	✓			NA
MRI findings	NA	NA	NA	NA	NA	NA	NA	✓	✓	✓	✓		✓	✓

Abbreviations: C = congenital; FTT = failure to thrive; LD = learning disabilities; NA = not applicable; OB = obesity; PN = postnatal.

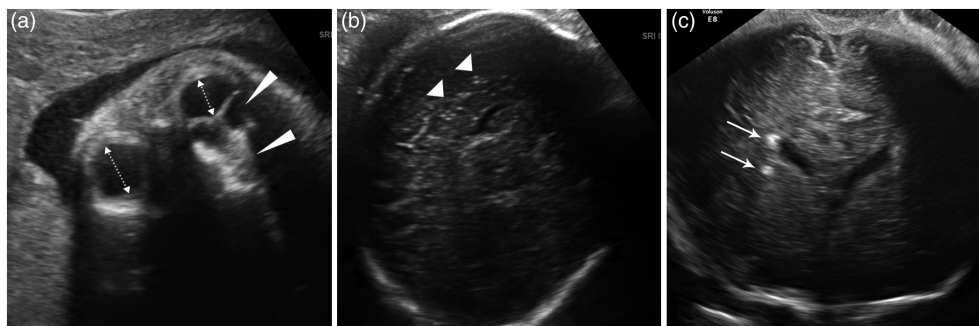


FIGURE 1 (a) Patient 1. Ultrasound image of the fetal eyes and orbits. The fetal left eye is smaller (dashed arrows) and compressed by a solid and cystic tumor within the posterior orbit (long arrowheads). (b) Patient 1. Retrospective evaluation of the US images showed on the parasagittal view of the brain clusters of small periventricular echogenic foci (white arrowheads). (c) Patient 2. Coronal view of the fetal brain. Periventricular echogenic foci near the anterior horns (arrows). See text for further details

tissue, and excessive number of sacral vertebrae where diagnosed with absence of posterior elements. Brainstem Auditory Evoked Response showed mild bilateral neurosensory hearing deficit. A renal scan showed unilateral mild hydronephrosis.

The child was referred for evaluation at our neuro-genetic clinic at the age of 21 months. Both weight and height were 4 SD below the mean for age, with a head circumference at the 15th percentile. The physical exam showed axial hypotonia, strabismus, and dysmorphic features including frontal bossing, upslanting palpebral fissures, small nose with depressed nasal bridge, and pectus excavatum. The developmental assessment demonstrated global developmental delay (DQ 52); the boy could crawl, sit steadily, and stand with support, but he was not able to sit or stand up by himself. He could mumble a variety of consonants and understood simple commands, but he did not pronounce any syllables.

3 | RESULTS

WES analysis in patient I-3 revealed a novel homozygous variant in *PRMT7*: c.1074_1075delAG: p.Arg358fs*9 (NM_001290018.1). This is a truncating variant which was found in two heterozygous carriers; 2/33575 Latino individuals in gnomAD (MAF 0.005957%) and in 2/245844 (MAF 0.00081%) of all populations. All other variants identified by exome sequencing were ruled out including variants in genes

associated with tumorigenesis. The variant was validated by Sanger sequencing performed at our clinical lab. Family segregation showed that both parents are heterozygous carriers for the same mutation and their older healthy 6-year-old son is not a carrier. Further analysis of the DNA sample obtained from the fetus described in patient I-2 found that the fetus was homozygous for the same variant (Figures 3 and 4).

4 | DISCUSSION

We describe the prenatal presentation of two male sibs, harboring a homozygous *PRMT7* mutation. Both fetuses presented with an early intrauterine growth restriction (IUGR), short long bones with normal shape and echogenicity, and nonspecific brain calcifications. Nevertheless, a rare optic nerve tumor was the prominent pathologic finding in the first fetus, versus a systemic venous anomaly in the second. The live born baby showed failure to thrive (both height and weight were 4 SD below the norm), hypotonia, strabismus, sensorineural hearing loss, genitourinary and skeletal involvement, anomalous venous drainage in the brain, global developmental delay, and dysmorphic features that included frontal bossing, upslanting palpebral fissures, small nose with depressed nasal bridge, and pectus excavatum.

The *PRMT7* gene, located on chromosome 16, encodes a member of the protein arginine *N*-methyltransferase family of proteins. This enzyme catalyzes the transfer of methyl groups from S-adenosyl-L-

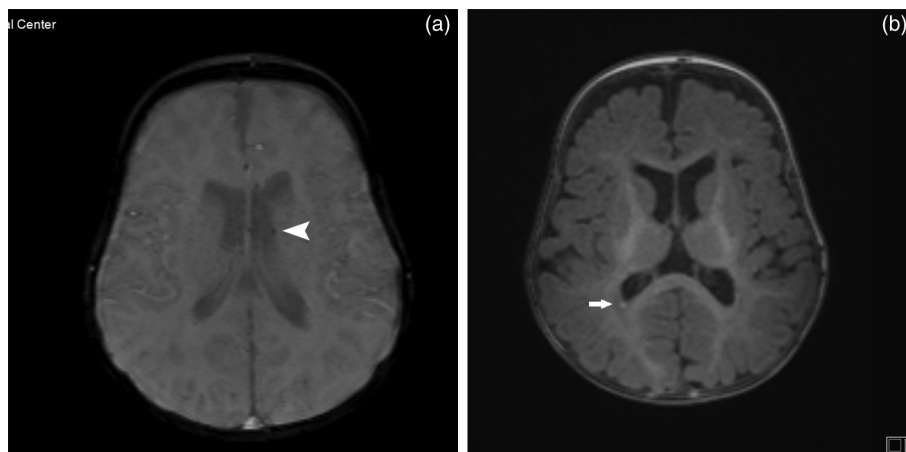


FIGURE 2 Patient 2, brain MRI at 7 months showing periventricular calcifications (a) arrowhead; (b) small arrow near the occipital horn

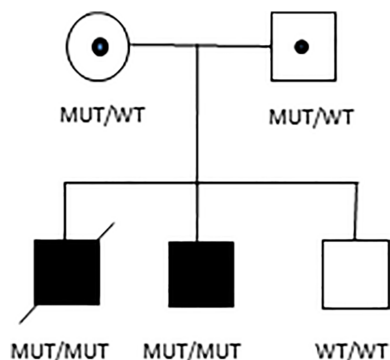


FIGURE 3 The family's pedigree [Color figure can be viewed at wileyonlinelibrary.com]

methionine to nitrogen atoms on arginine residues of different proteins, hence, exponentially expanding their functional complement. The methyltransferases regulate several cellular processes including signal transduction, RNA processing, DNA repair, protein subcellular localization, and interactions (Bedford & Clarke, 2009; Bedford & Richard, 2005). *PRMT7* function has been described in histone arginine methylation (Karkhanis et al., 2012; Migliori et al., 2012) and in the Wnt pathway (the latter may explain the skeletal involvement in our patients; Bikkavilli et al., 2012). The PRMT group contains nine members, but to date only mutations in *PRMT7* are known to cause a clinically relevant phenotype.

Eleven children with recessive mutations in the *PRMT7* gene were reported so far, as described in Table 1 (Agolini et al., 2018; Akawi et al., 2015; Kernohan et al., 2017; Valenzuela et al., 2018). They all shared the phenotypic features including short stature, hypotonia, brachydactyly, and mild to severe intellectual disability. Fetal US identified in two of the patients IUGR and polyhydramnios, and IUGR without polyhydramnios in another, postnatal exam demonstrated hypotonia in all but one, and microcephaly in five of them. Seizures were noted in six patients. Obesity or FTT were described in seven. All patients had dysmorphism including high forehead, hypertelorism, deep-set eyes, anteverted nares, thick lower lip, and short neck. Subsequently, a new clinical entity termed SBIDDS syndrome (short stature, brachydactyly, intellectual developmental disability, and seizures) was suggested for patients with *PRMT7* mutations (Akawi et al., 2015; Kernohan et al., 2017). Table 1 summarizes the common clinical features and the molecular data of these 11 patients, with the addition of the two patients we describe. The most common shared characteristics among these patients are hypotonia, dysmorphism (mainly deep-set eyes, long philtrum, and thin upper lip), short stature, brachydactyly, and developmental delay. The brain MRI findings are scarce, and need further characterization. A rare optic nerve tumor was the prominent pathologic finding in the first fetus and interestingly, the patient described by Valenzuela et al. (2018) had an orbital venous malformation in the extracorneal space.

The frame-shift variant detected in the two patients, p. Arg358fs*9, is located at the beginning of the C-terminal domain hence predicted to abolish the unique C-terminal domain of *PRMT7* protein. The eight different pathogenic variants found in the previously described patients are located both at the N-terminal and the C-terminal domains (Figure 5, Table 1). Agolini et al. (2018) suggest that

a more severe phenotype seems to be related with the presence of presence of null alleles. The mutation found in our patients is a null mutation, and they do present with quite a severe phenotype.

Our patients provide additional clinical data, expanding the phenotypic manifestations associated with mutations in *PRMT7*. These include brain calcifications and delayed myelination, sensorineural hearing impairment, anomalous venous drainage in the brain, and a congenital tumor, which, to the best of our knowledge, have not been previously described. These findings highlight two features that have not yet been associated with *PRMT7* mutations: the first is the brain calcifications and delayed myelination that may represent TORCH-like findings similar to those seen in Aicardi-Goutieres syndrome (AGS), which is a genetic immune-mediated disorder. Furthermore, the child had neonatal thrombocytopenia and developed sensorineural deafness which are also features seen in congenital CMV infection. Brain calcifications, leukoencephalopathy, and cerebral atrophy are the classic hallmarks of AGS (Stephenson, 2008). The AGS associated genes are involved in nucleic acid metabolism or signaling which, when mutated, can trigger a reaction similar to that in response to a viral infection and some patients have supporting data in the form of an

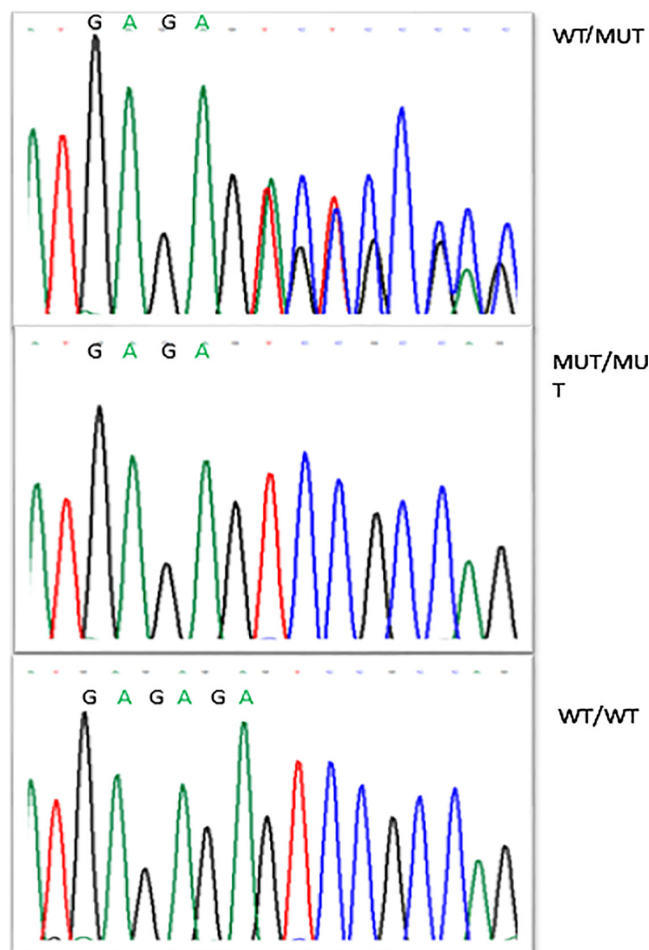


FIGURE 4 Sanger sequencing. The proband and the fetus are homozygous c.[1074_1075delAG];[1074_1075del AG]. The parents are heterozygous carriers c.[1074_1075delAG];[1074_1075=] and their older healthy old son is a noncarrier [Color figure can be viewed at wileyonlinelibrary.com]

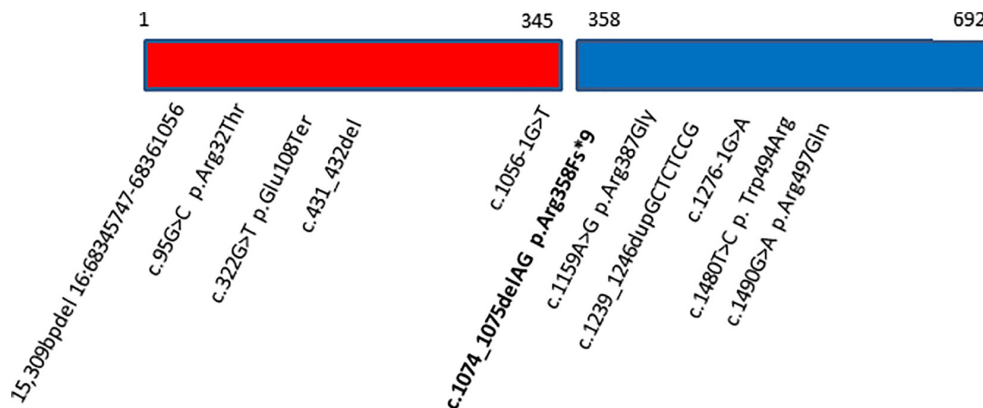


FIGURE 5 Protein domain structure of PRMT7 (692 amino acids) encompassing the N-terminal domain (14–345 in red) and the C-terminal domain (358–684 in blue). Yellow spots indicate the position of the pathogenic variants, the yellow arrow indicates the position of the deletion encompassing the transcription start site of PRMT7, the new mutation described here is bold [Color figure can be viewed at wileyonlinelibrary.com]

interferon signature (Crow & Manel, 2015). Thus, the *PRMT7* gene may also play a role in the immune system.

The second unique feature is the prenatal diagnosis of PA in the first patient. Glial cells are a group of cells consisting of astrocytes, oligodendrocytes, and ependymal cells from which various tumors may evolve, generally termed gliomas. Gliomas are traditionally grouped into either low or high grade (Swaiman, 2017). Pediatric low-grade gliomas (PLGG) represent the most common brain tumor in childhood, and are considered as Grade 1 or 2 according to the World Health Organization (Louis et al., 2016). PA is a Grade 1 PLGG that accounts, in the United States, for 17.4% of all primary CNS tumors in children aged 0–14 years (Ostrom et al., 2014). According to one population-based study (Burkhard et al., 2003), they may be located in the cerebellum (42%), supratentorial locations (36%), optic pathway and hypothalamus (9%), brainstem (9%), and spinal cord (2%). Typical elongated tumor cells, immune reactive to GFAP are among the characteristic features as was found in our patients (Collins, Jones, & Giannini, 2015). Interestingly, PA is diagnosed in 5–25% of patients with neurofibromatosis Type 1, and may involve the optic nerve, chiasm, optic tract, and hypothalamus (Kinori, Hodgson, & Zeid, 2018). Fetal and neonatal brain tumors are a rare entity. According to one review, of all childhood brain tumors, the ones diagnosed within the first 2 months after birth account for approximately 0.5–1.5% of patients (Rickert, 1999). In a literature review of 101 fetal and neonatal patients of astrocytoma, 9.9% were low grade astrocytoma located at the spinal cord (half of patients), cerebral hemisphere ($n = 3$), and optic nerve ($n = 2$; Isaacs, 2016). The role of *PRMT7* in tumorigenesis is highlighted in a recently published article describing arginine methylation in B cell histones by *PRMT7* (Ying et al., 2015). Reduced expression of *PRMT7* was associated with increased *Bcl6* levels. *Bcl6* takes part in regulation of apoptosis and differentiation. Previous studies have shown that increased *Bcl6* levels are linked with tumorigenesis. Interestingly, an association has been emphasized between increased *Bcl6* levels and astrocytomas (Ruggieri et al., 2014). In addition, *PRMT7* gene variations were found to be involved in breast cancer metastasis (Geng et al., 2017; Yao et al., 2014). Thus patients with

PRMT7 mutations may be at increased risk for malignancies involving the brain and other organs.

In conclusion, in patients with prenatal demonstration of FGR with short long bones and calcified brain parenchyma NGS should be offered. Once, mutations in *PRMT7* are found, prenatal counseling of an unfavorable neurodevelopmental outcome, sensorineural hearing loss, and dysmorphic and skeletal features.

ACKNOWLEDGMENT

The authors wish to thank the family for their cooperation and permission to publish.

CONFLICT OF INTEREST

The authors have no conflicts of interest to report.

ORCID

Dorit Lev  <https://orcid.org/0000-0001-6869-6727>

REFERENCES

- Agolini, E., Dentici, M. L., Bellacchio, E., Alesi, V., Radio, F. C., Torella, A., ... Novelli, A. (2018). Expanding the clinical and molecular spectrum of *PRMT7* mutations: Three additional patients and review. *Clinical Genetics*, 93, 675–681. <https://doi.org/10.1111/cge.13137>
- Akawi, N., McRae, J., Ansari, M., Balasubramanian, M., Blyth, M., Brady, A. F., ... DDD study. (2015). Discovery of four recessive developmental disorders using probabilistic genotype and phenotype matching among 4,125 families. *Nature Genetics*, 47, 1363–1369. <https://doi.org/10.1038/ng.3410>
- Bedford, M. T., & Clarke, S. G. (2009). Protein arginine methylation in mammals: Who, what, and why. *Molecular Cell*, 33, 1–13. <https://doi.org/10.1016/j.molcel.2008.12.013>
- Bedford, M. T., & Richard, S. (2005). Arginine methylation an emerging regulator of protein function. *Molecular Cell*, 18, 263–272.
- Bikkavilli, R. K., Avasarala, S., Vanscoyk, M., Sechler, M., Kelley, N., Malbon, C. C., & Winn, R. A. (2012). Dishevelled3 is a novel arginine methyl transferase substrate. *Scientific Reports*, 2, 805. <https://doi.org/10.1038/srep00805>

- Burkhard, C., Di Patre, P. L., Schüler, D., Schüler, G., Yaşargil, M. G., Yonekawa, Y., ... Ohgaki, H. (2003). A population-based study of the incidence and survival rates in patients with pilocytic astrocytoma. *Journal of Neurosurgery*, *98*, 1170–1174.
- Chitty, L. S., & Altman, D. G. (2002). Charts of fetal size: Limb bones. *BJOG*, *109*, 919–929.
- Collins, V. P., Jones, D. T., & Giannini, C. (2015). Pilocytic astrocytoma: Pathology, molecular mechanisms and markers. *Acta Neuropathologica*, *129*, 775–788. <https://doi.org/10.1007/s00401-015-1410-7>
- Crow, Y. J., & Manel, N. (2015). Aicardi-Goutières syndrome and the type I interferonopathies. *Nature Reviews. Immunology*, *15*, 429–440. <https://doi.org/10.1038/nri3850>
- Geng, P., Zhang, Y., Liu, X., Zhang, N., Liu, Y., Liu, X., ... Lu, J. (2017). Auto-methylation of protein arginine methyltransferase 7 and its impact on breast cancer progression. *The FASEB Journal*, *31*, 2287–2300. <https://doi.org/10.1096/fj.201601196R>
- Hadlock, F. P., Harrist, R. B., Shah, Y. P., Sharman, R. S., & Park, S. K. (1990). Sonographic fetal growth standards. Are current data applicable to a racially mixed population? *J Ultrasound Med.* (3), 157–60.
- Isaacs, H., Jr. (2016). Perinatal (fetal and neonatal) astrocytoma: A review. *Child's Nervous System*, *32*, 2085–2096.
- Karkhanian, V., Wang, L., Tae, S., Hu, Y. J., Imbalzano, A. N., & Sif, S. (2012). Protein arginine methyltransferase 7 regulates cellular response to DNA damage by methylating promoter histones H2A and H4 of the polymerase delta catalytic subunit gene, POLD1. *The Journal of Biological Chemistry*, *287*, 29801–29814. <https://doi.org/10.1074/jbc.M112.378281>
- Kernohan, K. D., McBride, A., Xi, Y., Martin, N., Schwartzentruber, J., Dymont, D. A., ... Chitayat, D. (2017). Loss of the arginine methyltransferase PRMT7 causes syndromic intellectual disability with microcephaly and brachydactyly. *Clinical Genetics*, *91*, 708–716. <https://doi.org/10.1111/cge.12884>
- Kinori, M., Hodgson, N., & Zeid, J. L. (2018). Ophthalmic manifestations in neurofibromatosis type 1. *Survey of Ophthalmology*, *63*, 518–533. <https://doi.org/10.1016/j.survophthal.2017.10.007>
- Louis, D. N., Perry, A., Reifenberger, G., von Deimling, A., Figarella-Branger, D., Cavenee, W. K., ... Ellison, D. W. (2016). The 2016 World Health Organization classification of tumors of the central nervous system: A summary. *Acta Neuropathologica*, *131*, 803–820. <https://doi.org/10.1007/s00401-016-1545-1>
- Migliori, V., Müller, J., Phalke, S., Low, D., Bezzi, M., Mok, W. C., ... Guccione, E. (2012). Symmetric dimethylation of H3R2 is a newly identified histone mark that supports euchromatin maintenance. *Nature Structural & Molecular Biology*, *19*, 136–144. <https://doi.org/10.1038/nsmb.2209>
- Ostrom, Q. T., Gittleman, H., Liao, P., Rouse, C., Chen, Y., Dowling, J., ... Barnholtz-Sloan, J. (2014). CBTRUS statistical report: Primary brain and central nervous system tumors diagnosed in the United States in 2007–2011. *Neuro-Oncology*, *16*(Suppl 4), iv1–iv63. <https://doi.org/10.1093/neuonc/nou223>
- Rickert, C. H. (1999). Neuropathology and prognosis of foetal brain tumours. *Acta Neuropathologica*, *98*, 567–576.
- Ruggieri, S., Tamma, R., Marzullo, A., Annese, T., Marinaccio, C., Errede, M., ... Nico, B. (2014). Translocation of the protooncogene Bcl-6 in human glioblastoma multiforme. *Cancer Letters*, *353*, 41–51. <https://doi.org/10.1016/j.canlet.2014.06.017>
- Stephenson, J. B. (2008). Aicardi-Goutières syndrome (AGS). *European Journal of Paediatric Neurology*, *12*, 355–358. <https://doi.org/10.1016/j.ejpn.2007.11.010>
- Swaiman, K. F. (2017). *Swaiman's pediatric neurology: Principles and practice* (6th ed.). Edinburgh: Elsevier.
- Valenzuela, I., Segura-Puimedon, M., Rodríguez-Santiago, B., Fernández-Alvarez, P., Vendrell, T., Armengol, L., & Tizzano, E. (2018). Further delineation of the phenotype caused by loss of function mutations in PRMT7. *European Journal of Medical Genetics*, *S1769-7212*(17), 30691–30692. <https://doi.org/10.1016/j.ejmg.2018.07.007>
- Yao, R., Jiang, H., Ma, Y., Wang, L., Wang, L., Du, J., ... Lu, J. (2014). PRMT7 induces epithelial-to-mesenchymal transition and promotes metastasis in breast cancer. *Cancer Research*, *74*, 5656–5667. <https://doi.org/10.1158/0008-5472.CAN-14-0800>
- Ying, Z., Mei, M., Zhang, P., Liu, C., He, H., Gao, F., & Bao, S. (2015). Histone arginine methylation by PRMT7 controls germinal center formation via regulating Bcl6 transcription. *Journal of Immunology*, *195*(4), 1538–1547.

How to cite this article: Birnbaum R, Yosha-Orpaz N, Yanoov-Sharav M, et al. Prenatal and postnatal presentation of PRMT7 related syndrome: Expanding the phenotypic manifestations. *Am J Med Genet Part A*. 2019;179A:78–84. <https://doi.org/10.1002/ajmg.a.6>